Exploring Localization Properties in a Folded N x N Network on a Cylinder's shape with diagonal Disorder and Long-Range Hopping

M. S. Santos Junior[1], F. A. B. F. de Moura[1]

[1] *Instituto de Física, Universidade Federal de Alagoas, 57072-900 Maceió, Alagoas, Brazil*

Abstract

In this work, we employ the inverse power method (IPM), a well-established technique in linear algebra, to investigate the quantum dynamics of a one-electron Hamiltonian in a unique geometric setup. Specifically, we consider a two-dimensional $N \times N$ lattice folded into a cylindrical topology, incorporating diagonal disorder and long-range hopping with a power-law decay. Unlike conventional studies that consider two-dimensional planar lattices, our model explicitly incorporates the curvature of the cylindrical geometry, enabling us to examine its potential influence on electronic properties. By analyzing the interplay between disorder, long-range hopping, and the system's intrinsic curvature, our results suggest that geometry may play a role in the localization and transport behavior of electrons. These findings provide insights into how geometric factors could affect quantum systems, with potential implications for materials science and nanostructures exhibiting curved geometries.

Keywords: localization ; inverse power method ; long-range hopping

1. Introduction

In recent decades, the scientific community has shown a significant interest in electronic transport in systems with various topologies, including linear, two-dimensional, or three-dimensional lattices. Particularly noteworthy are quasi-one-dimensional systems, where one or two dimensions are much smaller than the third, as they exhibit intriguing transport properties [1, 2, 3]. Similar behaviors can also arise in quasi-two-dimensional systems [4, 5, 6].

The literature contains numerous studies involving systems with cylindrical geometry. For instance, in reference [7], the authors conducted a survey of

the interaction between two cylinders in a flow environment, employing computational simulations and experimental analyses. Other works, such as [8], discuss enhancements in heat transport in nanometric alumina–copper/water hybrid fluids flowing over stretched cylinders. Additionally, research has been conducted to investigate the phase diagram of the ground state of the Hubbard model doped in a four-leg cylinder. Here, the Hubbard model theoretically represents the interaction between electrons and solids, while doping refers to the controlled introduction of charge carriers into the system under study [9]. Reference [10] addresses the localization effect in a synthetic Hall cylinder, where this phenomenon arises from the interaction between waves due to disorder and dispersion, resulting in concentration in specific regions of the system. This study explores this phenomenon in a synthetic scenario, employing a Hall cylinder as a test platform.

Anderson Localization theory [11] is currently under extensive study. In reference [12], the authors investigated spectral function distributions using the correlated Anderson model. Unlike previous works that focused solely on analyzing the mean of the spectral function, neglecting its distribution, this study examines the distribution of the spectral function in systems with electronic correlations. In another study [13], the effect of long-range correlated disorder on localization properties in mixed transmission lines was explored. These lines are physical systems consisting of multiple paths through which waves, such as electrons in conductive materials or photons in optical media, can be transmitted. The research investigates how the presence of two independent sources of long-range correlated clutter affects wave localization along mixed transmission lines. Recent work has explored how correlated disorder [14, 15] can enhance the robustness of superconductivity in certain systems [16]. The authors theoretically examined how different configurations of correlated disorder influence the superconducting properties of materials. Reference [17] investigated the phenomenon of localization in random fractal lattices, complex geometric structures exhibiting self-similarity at different scales, and examined how the combination of disorder and fractal geometry affects the localization properties of waves or particles propagating through these lattices.

Reference [18] delves into the localization of a lattice operator with long-range hopping, modeled by a polynomial, in the presence of uniform electric fields. This research investigates how the combination of long-range hopping and uniform electric fields affects the localization properties of particles moving within the lattice. In one-dimensional systems [19], or two-dimensional

systems, quantum transport with long-range hopping has been explored under various conditions, such as different lattice geometries and magnetic field strengths [20]. In three-dimensional systems, research has focused on studying how anisotropy in long-range hopping affects the localization phenomenon [21].

In this study, we investigate a system consisting of an $N \times N$ lattice folded into a cylindrical geometry, incorporating diagonal disorder and long-range hopping interactions with a power-law decay. The Hamiltonian governing the electron dynamics in this system explicitly accounts for the effects of the curved geometry, allowing us to study the interplay between disorder, long-range interactions, and topology. In summary, we write the standard one-electron Hamiltonian with long-range hopping directly on a cylindrical structure with height N and perimeter N. Our investigation reveals how the combined effects of disorder, geometry and long-range hopping influence localization-delocalization transitions and transport properties. These transitions, shaped by the cylindrical geometry, provide insights into the fundamental mechanisms governing electronic states in disordered systems. Such insights are crucial for extending theoretical models to curved geometries and can have broader implications for nanostructures and materials where disorder and topology play significant roles. The paper is organized as follows: First, we describe the system's topology and present the Hamiltonian that incorporates both long-range hopping and diagonal disorder. Next, we outline the numerical methods employed, including the inverse power method (IPM), to solve the quantum Hamiltonian and analyze its properties. Finally, we present our results, discuss their implications, and highlight the novel insights gained from studying this model.

2. Model and formalism

Our model is a $N \times N$ grid in a cylinder shape. Each point i, j of this grid represents a single electron orbital $|R_{i,j}\rangle$. Therefore, the radius of this cylinder is $r = N/2\pi$. The angular distance between sites is $\theta = 2\pi/N$. Therefore, the coordinates of each site i are given by : $x_{i,j} = -r\cos[(j-1)\theta]$, $y_{i,j} = r\sin[(j-1)\theta]$ and $z_{i,j} = i$. We emphasize that the z-direction of the cylinder has open boundary conditions. By using the above topology, we can write the Hamiltonian as

$$H = \sum_{i,j} \epsilon_{i,j} |R_{i,j}\rangle \langle R_{i,j}| + \sum_{ij,op} J_{ij,op} |R_{i,j}\rangle \langle R_{o,p}| , \tag{1}$$

where $|R_{i,j}\rangle$ is the vector ket of a state at position $\mathbf{R}_{i,j} = (x_{i,j}, y_{i,j}, z_{i,j})$ with on-site energy $\epsilon_{i,j}$. These energies are taken as random and uncorrelated for different sites and distributed uniformly around zero within the interval $[-4, 4]$. The hopping $J_{ij,op}$ do not fluctuate and are set in the form $J_{ij,op} = 1/|\mathbf{R}_{i,j} - \mathbf{R}_{o,p}|^{\nu}$, with $i, j \neq o, p$. We emphasize that the amount of disorder considered here is in the same order as the bandwidth of this Hamiltonian. Therefore, we deal with a degree of intermediate (or almost strong) disorder. We are interested in investigating the effect of cylinder topology on the nature of eigenstates and the statistical properties within the present model. We emphasize that based on the previous literature [22, 23, 24], models with power decay hopping terms exhibit an asymmetric spectrum where the largest eigenvalue, in general, can have its localization degree influenced by the long-range interaction. Therefore, the wanted localization properties will appear at the last eigenstate. We can focus our main numerical tools on finding only the largest eigenvalue and its respective eigenvector. We will do it using the inverse power method (IPM) [25]. This procedure is an iterative numerical technique to find the largest eigenvalue of the Hermitian matrix H. The method can be explained as follows: i) initially, we start by considering a general wave-state $|\Phi^0\rangle = \sum_{i,j} \phi^0_{i,j} |R_{i,j}\rangle$ where, for example, $\phi^0_{i,j} = 1/(N^2)$. ii) We calculate then the following new wave-vector defined as $|\Phi^1\rangle = H |\Phi^0\rangle$. We normalized this vector as $|\overline{\Phi^1}\rangle = |\Phi^1\rangle / ||\Phi^1\rangle|^2$. iii) We calculate the new wave-state defined as: $|\Theta\rangle = H |\overline{\Phi^1}\rangle$. iv) We calculate the quantity $E^1_M = \langle\Theta|\overline{\Phi^1}\rangle$. We can exchange $|\Phi^0\rangle$ by $|\overline{\Phi^1}\rangle$ and repeat the procedure (i-iv) recursively k times. The final values found (E^k_M and $|\overline{\Phi^k}\rangle$) will converge respectively to the largest eigenvalue and his eigenstate. The convergence of the method can be monitored using the values of E_M in two subsequent iterations, i.e., the iterative process will stop when $|E^k_M - E^{k-1}_M| < 10^{-8}$. Therefore, after applying the procedure outlined above, we will find the largest eigenvalue and the respective eigenstate $|\overline{\Phi^k}\rangle = \sum_{i,j} \overline{\phi^k_{i,j}} |i, j>$. To understand the localization properties of this state, we will explore the size dependence and the statistical fluctuations of the participation number. The participation number for this state is given by [26]:

$$P_k = \left(\sum_{i,j=1}^{N} |\overline{\phi^k_{i,j}}|^4 \right)^{-1} \tag{2}$$

Our main calculations will be performed using the average participation number, defined as $P = \langle P_k \rangle_s$, where $\langle \ldots \rangle_s$ represents an average over a large

number of samples s ($s > 1000$). We also calculate two metrics defined as: $M_2 = [\sqrt{P^2}]/P$ and $M_3 = [(P^3)^{1/3}]/P$, where $P^2 = \langle P_k^2 \rangle_s$ and $P^3 = \langle P_k^3 \rangle_s$. For extended states, the fluctuations of the participation number are well controlled [24] and both $[\sqrt{P^2}]$ and $[(P^3)^{1/3}]$ are roughly similar to P, therefore, we have $M_2 \approx M_3 \approx 1$. However, for localized states, the fluctuations of the participation number increase as N increases and thus both M_2 and M_3 should also increase. We will study the dependence of P on ν and its finite size scaling. Our research aims to determine whether or not any extended states are present in this disordered cylinder geometry. It's important to note that in disordered chains ($d = 1$) or disordered planes ($d = 2$), references [22, 23, 24] have demonstrated that extended states could be seen at the end of the spectrum when $d < \nu < 3d/2$. We are interested in investigating the effect of cylinder topology on the nature of eigenstates and the statistical properties within the present model.

3. Results

In our study, we employ the previously described inverse power method on $N \times N$ networks with N up to 180 sites. During our numerical experiments, we manage the numerical precision of the largest eigenvalue by evaluating values obtained in successive iterations. The discrepancy between eigenvalues in consecutive iterations was approximately 10^{-8}. Our method proved to be reasonably efficient, achieving convergence within fewer than $k = 200$ iterations. Following the computation of the largest eigenvalue and its corresponding eigenvector, we verify the maintenance of the secular equation ($H\,|\overline{\Phi^k}\rangle = E^k\,|\overline{\Phi^k}\rangle$). Our tests exhibited errors smaller than 10^{-8} for all considered values of N. Figure 1(a) depicts the scaled participation number (P/N^2) plotted against the exponent ν for various chain sizes ($N = 60, 90, 120, 150, 180$). The results presented illustrate that for $\nu \leq 2.80$, the rescaled participation P/N^2 remains relatively constant, indicating an extended state. Conversely, for $\nu > 2.8$, the rescaled participation decreases with increasing N, suggesting localization of the state in this regime. In Figures 1(b) and (c), M_2 and M_3 are plotted against ν for the same chain sizes. The primary findings remain consistent: extended states are observed for $\nu \leq 2.8$, while localized modes emerge for $\nu > 2.8$.

Figure 2(a) displays the mean participation versus N for all values of ν considered. The results indicate that for large ν, the participation shows little dependence on N; conversely, for small ν, the participation increases

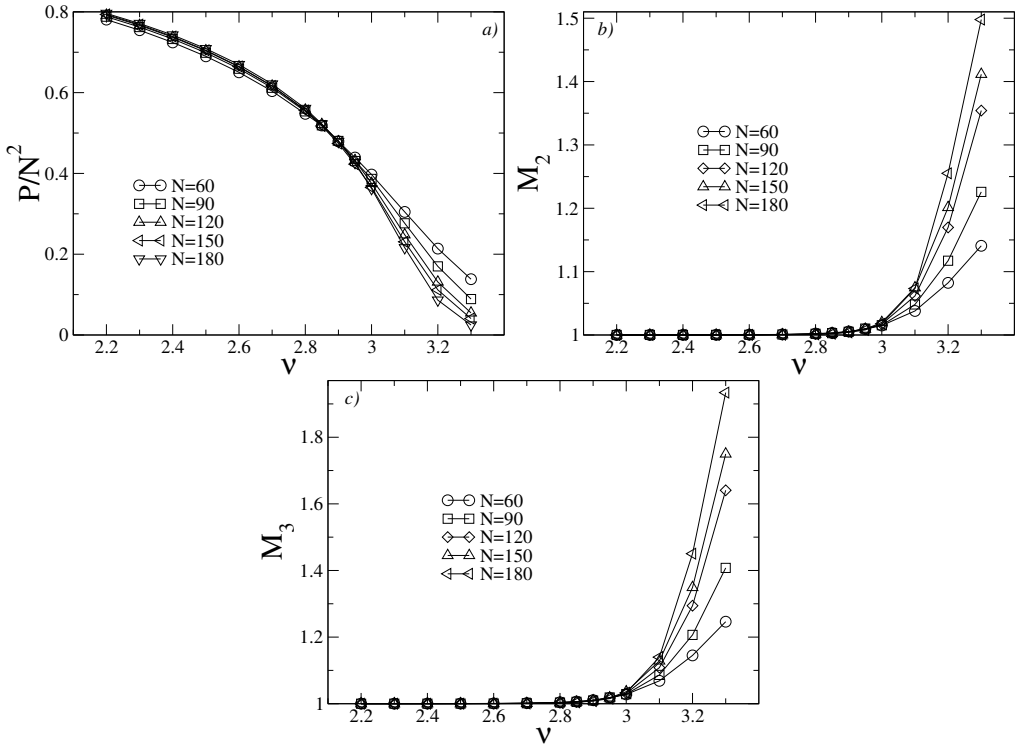

Figure 1: a) The scaled participation number (P/N^2) versus the exponent ν for $N = 60, 90, 120, 150, 180$. b) M_2 versus ν and c) M_3 versus ν for the same cases considered in (a).

with N. These findings agree with the results presented in figure 1. We will employ rescaled variables ($P^2/N^2 \times \zeta^2/N^2$) to construct a collapse of all this data onto a single curve. Figure 2(b) illustrates this collapse of all data onto a single curve. The parameter ζ is a characteristic length of the system that depends on the exponent ν. For $\nu >> 2.8$ the scaled participation number P^2/N^2 becomes a small values roughly proportional to ζ^2/N^2 (thus $P \approx$ constant). For $\nu \leq 2.8$, the collapse function becomes roughly a constant, thus $P \approx N^2$. The dependence of ζ on ν can be observed in figure 2(c). The numerical error at the estimates of ζ is the order of the symbol's size. This figure shows two branches: the lower branch, representing values of ν between 2.85 and 3.3, corresponds to the localized branch. The upper branch, representing the region of ν smaller than 2.85, corresponds to the extended branch. Let's analyze the behavior of ζ near the transition, i.e.,

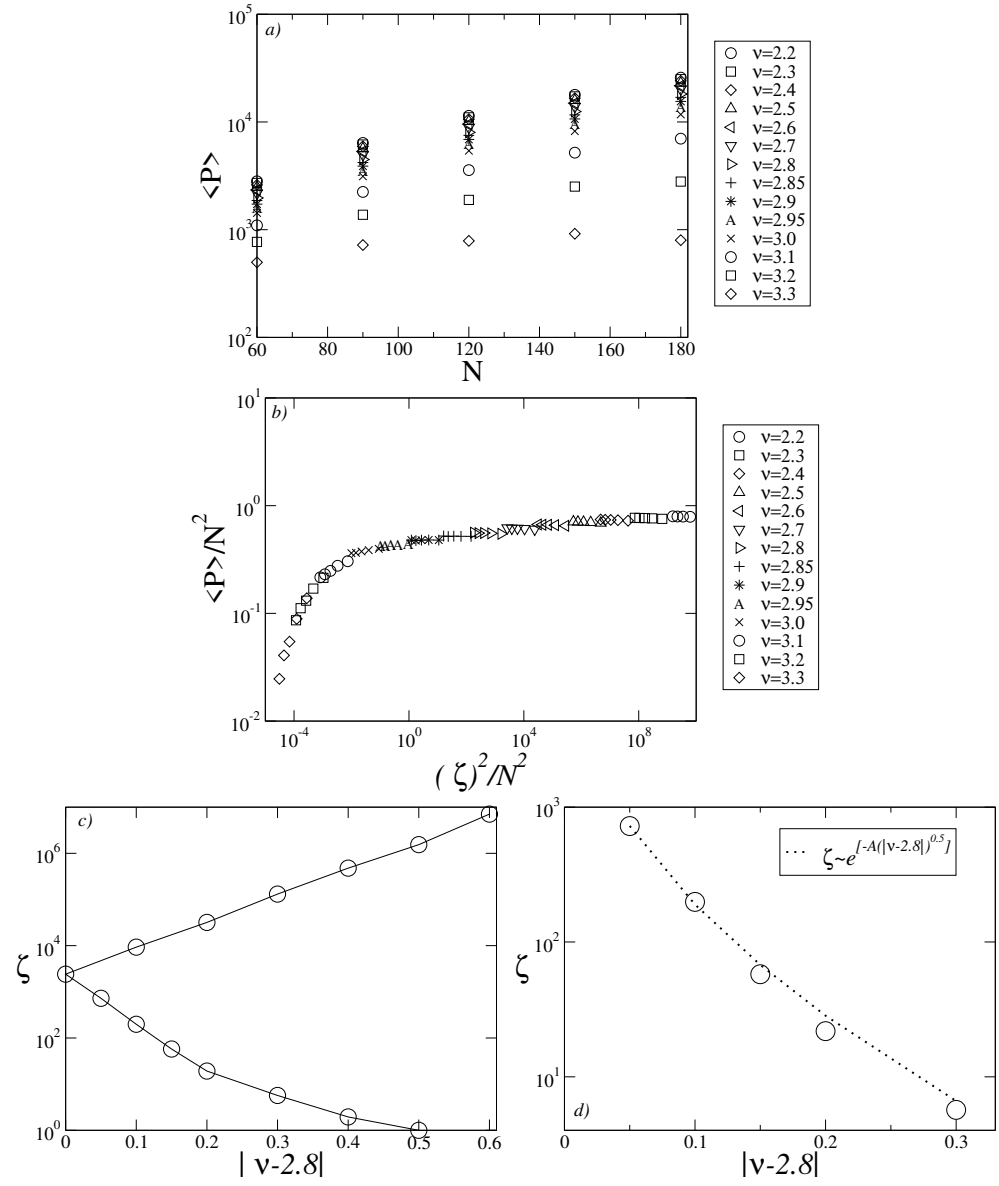

Figure 2: a) Mean participation versus N for $\nu = 2.1$ up to 3.3. b) A data collapse of all data using the scaled variables P/N^2 versus ζ^2/N^2. c) The characteristics lenght ζ versus $|\nu - 2.8|$ for all values of ν. d) ζ versus $|\nu - 2.8|$ for $\nu > 2.8$ (i.e., the localized branch) suggests an exponential profile $\zeta \propto e^{[-A\sqrt{|\nu-2.8|}]}$ with $A > 0$.

for ν slightly more significant than 2.8. By examining the data around this region, we observe that the characteristic length ζ exhibits an exponential behavior such $\zeta \propto e^{[-A\sqrt{|\nu-2.8|}]}$ with $A > 0$. Our calculations suggest that this model contains only localized states for $\nu > 2.8$. For $\nu \leq 2.8$, our results suggest that the largest eigenvalue extends with the participation number proportional to N^2. The phase transition around $\nu = 2.8$ exhibits an exponential increase in the characteristic localization length. Our main results indicate that the largest eigenvalue becomes extended for $2 < \nu \leq 2.8$. For $\nu > 2.8$, our results suggest that all eigenstates become localized. As the intensity of the long-range decay (ν) approaches the critical point, the characteristic localization length seems to exhibit an exponential divergence. The existence of a class of exponential behaviors on the characteristic size scales is also present, for example, in models with Kosterlitz-Thouless-like transition[27].

Compared with previous works that investigated disordered plane grids [22], our results reveal that the transition point here ($\nu \approx 2.8$) is slightly smaller than the value found there ($\nu = 3$). One possible indication of this difference is the cylindrical geometry. The distances between sites within the actual topology are different from those considered in [22], which may play a relevant role in the critical properties. However, we must be honest and acknowledge that this discrepancy could also be an effect of finite-size effects. Indeed, there is, of course, the possibility that if we consider $N \gg 180$, the transition point we obtained (2.8) could shift slightly. Before concluding our work, we would like to briefly comment on the intensity of the disorder we have considered. We emphasize that the disorder magnitude ($[-4, 4]$) is of the same order as the energy band. We also performed some experiments with disorder widths slightly different from this range, and the results were qualitatively the same. For weaker disorder (e.g., $[-2, 2]$ or smaller), the system size needs to be increased, but we were unable to do this within our laboratory constraints. Nonetheless, we suspect that the main results will remain consistent for weaker disorders. By "main results," we mean the extended state at the largest eigenvalue for $\nu \leq 2.8$ and localized states for $\nu > 2.8$. The statistical properties of the transition around the critical point could, however, exhibit some changes.

4. Summary and final remarks

In this work, we applied the inverse power method (IPM) to analyze the behavior of disordered cylindrical networks of varying sizes, with up to 180 *sites. The precision of the largest eigenvalue was ensured through iterative refinement, achieving a convergence discrepancy of approximately* 10^{-8} *between consecutive eigenvalues. The method proved highly efficient, requiring fewer than 200 iterations for convergence. Validation against the secular equation confirmed errors smaller than* 10^{-8} *for all considered values of* N*, demonstrating the robustness of our approach. Our analysis of the scaled participation number* (P/N^2) *as a function of the exponent* ν *revealed a clear distinction between extended and localized states. For* $\nu \leq 2.80$*, the scaled participation remained relatively constant, signifying the presence of extended states. Conversely, for* $\nu > 2.80$*, scaled participation decreased with increasing* N*, indicating localization. By examining the mean participation as a function of* N*, we observed a dependence on* ν*, with rescaled variables collapsing the data onto a universal curve. The characteristic localization length* ζ *exhibited exponential scaling near the critical transition point (*$\nu \approx 2.80$*), suggesting a divergence consistent with a transition from extended to localized states. These findings highlight the interplay between disorder, long-range hopping, and cylindrical geometry, suggesting that extended states can exist in disordered cylindrical systems with intermediate diagonal disorder and long-range hopping interactions. The small difference in the critical transition value (*$\nu \approx 2.80$*) compared to the value* $\nu = 3$ *found in the literature may be related to the cylindrical geometry considered in our model, which differs fundamentally from the planar structures studied previously. However, we must also acknowledge that this discrepancy could be due to finite-size effects, as the largest system size we were able to consider in our computational environment was* $N = 180$*. However, it is important to emphasize that in many of the earlier studies [22] on localization properties in 2D planes with long-range hopping (with open or closed boundary conditions), the value of* N *was also on the order of 100–200 (in some cases, it slightly exceeded this range). In all these studies, the transition was found at* $\nu \approx 3$ *(considering system sizes similar to those used here). Therefore, the lower critical value obtained here (*$\nu \approx 2.8$*) is possibly related to the cylindrical geometry rather than finite-size effects.*

In conclusion, this work demonstrates the application of the inverse power method (IPM) to investigate the quantum dynamics of disordered cylindrical

networks. Our results provide insights into the interplay between disorder, long-range hopping, and geometric effects, revealing how these factors collectively influence localization-delocalization transitions in disordered systems. The identification of a critical transition point near $\nu \approx 2.80$, along with the observed scaling behavior, deepens our understanding of the fundamental mechanisms governing electronic states in curved geometries. Looking ahead, this study lays the foundation for future investigations into the impact of geometry and long-range interactions on disordered systems, with potential implications for the design of novel materials and nanostructures. By refining computational methods and exploring larger systems, we aim to further uncover the intricate roles that curvature, disorder, and topology play in the quantum transport properties of these systems.

5. Acknowledgments

This work was supported by CAPES (Coordenação de Aperfeiçoamento de Pessoal do Nível Superior), CNPq (Conselho Nacional de Densenvolvimento Científico e Tecnológico), and FAPEAL (Fundação de Apoio à Pesquisa do Estado de Alagoas).

References

[1] D.-S. Hu, S.-J. Xiong, The transport properties of quasi-one-dimensional double-chain systems in a magnetic field, Journal of Physics: Condensed Matter 12 (2000) 7933.

[2] A. Smontara, A. Bilušić, E. Tutiš, H. Berger, F. Levy, Effects of doping on the transport properties of the quasi-one-dimensional system (tase4) 2i, Synthetic Metals 103 (1999) 2663–2666.

[3] B. Kramer, J. Mašek, V. Špička, B. Velickỳ, Coherent electronic transport properties of quasi-one-dimensional systems, Surface Science 229 (1990) 316–320.

[4] Q. Wu, L. Shen, M. Yang, Y. Cai, Z. Huang, Y. P. Feng, et al., Electronic and transport properties of phosphorene nanoribbons, Physical Review B 92 (2015) 035436.

[5] T. Martins, R. H. Miwa, A. J. Da Silva, A. Fazzio, Electronic and transport properties of boron-doped graphene nanoribbons, Physical Review Letters 98 (2007) 196803.

[6] Z. Li, H. Qian, J. Wu, B.-L. Gu, W. Duan, Role of symmetry in the transport properties of graphene nanoribbons under bias, Physical Review Letters 100 (2008) 206802.

[7] L. Ding, Y. Han, Z. Yang, L. Zhang, H. He, Influence of upstream cylinder on flow-induced vibration and heat transfer of downstream cylinder, International Journal of Thermal Sciences 176 (2022) 107519.

[8] M. M. Maskeen, A. Zeeshan, O. U. Mehmood, M. Hassan, Heat transfer enhancement in hydromagnetic alumina–copper/water hybrid nanofluid flow over a stretching cylinder, Journal of Thermal Analysis and Calorimetry 138 (2019) 1127–1136.

[9] Y.-F. Jiang, J. Zaanen, T. P. Devereaux, H.-C. Jiang, Ground state phase diagram of the doped hubbard model on the four-leg cylinder, Physical Review Research 2 (2020) 033073.

[10] R. Zhang, Y. Yan, Q. Zhou, Localization on a synthetic hall cylinder, Physical Review Letters 126 (2021) 193001.

[11] P. W. Anderson, Absence of diffusion in certain random lattices, Physical Review 109 (1958) 1492.

[12] N. A. Khan, Spectral function distributions in the correlated anderson model, Chinese Journal of Physics 85 (2023) 733–740.

[13] E. Lazo, Influence of two independent sources with long-range correlated disorder in the localization properties of mixed transmission lines, Physica E: Low-dimensional Systems and Nanostructures 114 (2019) 113628.

[14] J. dos Santos, M. Sales, F. de Moura, Absorption spectra and localization aspects of a one-dimensional model with stretched exponential correlated disorder, Physica A: Statistical Mechanics and its Applications 413 (2014) 31–41.

[15] L. da Silva, A. R. Neto, M. Sales, M. Lyra, F. de Moura, Optical absorption and delocalization in a quaternary tight-binding chain with correlated disorder, Physica A: Statistical Mechanics and its Applications 486 (2017) 895–900.

[16] V. D. Neverov, A. E. Lukyanov, A. V. Krasavin, A. Vagov, M. D. Croitoru, Correlated disorder as a way towards robust superconductivity, Communications Physics 5 (2022) 177.

[17] A. Kosior, K. Sacha, Localization in random fractal lattices, Physical Review B 95 (2017) 104206.

[18] Y. Sun, C. Wang, Localization of polynomial long-range hopping lattice operator with uniform electric fields, Letters in Mathematical Physics 114 (2023) 6.

[19] J. C. Cressoni, M. L. Lyra, The nature of electronic states in a disordered chain with long-ranged hopping amplitudes, Physica A: Statistical Mechanics and its Applications 256 (1998) 18–29.

[20] S.-S. Wang, K. Li, Y.-M. Dai, H.-H. Wang, Y.-C. Zhang, Y.-Y. Zhang, Quantum transports in two-dimensions with long range hopping, Scientific Reports 13 (2023) 5763.

[21] J. T. Cantin, T. Xu, R. V. Krems, Effect of the anisotropy of long-range hopping on localization in three-dimensional lattices, Physical Review B 98 (2018) 014204.

[22] A. Rodríguez, V. A. Malyshev, G. Sierra, M. A. Martín-Delgado, J. Rodríguez-Laguna, F. Domínguez-Adame, Anderson transition in low-dimensional disordered systems driven by long-range nonrandom hopping, Phys. Rev. Lett. 90 (2003) 027404.

[23] A. V. Malyshev, V. A. Malyshev, F. Domínguez-Adame, Monitoring the localization-delocalization transition within a one-dimensional model with nonrandom long-range interaction, Phys. Rev. B 70 (2004) 172202.

[24] F. A. B. F. de Moura, A. V. Malyshev, M. L. Lyra, V. A. Malyshev, F. Domínguez-Adame, Localization properties of a one-dimensional tight-binding model with nonrandom long-range intersite interactions, Phys. Rev. B 71 (2005) 174203.

[25] R. Bronson, G. B. Costa, J. T. Saccoman, D. Gross, 4 - eigenvalues and eigenvectors, in: R. Bronson, G. B. Costa, J. T. Saccoman, D. Gross (Eds.), Linear Algebra (Fourth Edition), fourth edition Edition, Academic Press, Oxford, 2024, p. 243–284.

[26] R. F. Dutra, M. S. Santos Junior, D. Messias, C. V. C. Mendes, M. O. Sales, F. A. B. F. de Moura, Charge transport in two-dimensional disordered systems with an external electric field, International Journal of Modern Physics C 34 (08) (2023) 2350110.

[27] W. Dias, F. de Moura, M. Coutinho-Filho, M. Lyra, Kosterlitz–thouless-like transition in two-dimensional lattices with long-range correlated hopping terms, Physics Letters A 374 (2010) 3572–3575.